

Comparison of diluted antiferromagnetic Ising models on frustrated lattices in a magnetic field

Konstantin Soldatov^{1,2,*}, Alexey Peretyatko^{1,†}, Konstantin Nefedev^{1,2,‡} and Yutaka Okabe^{3§}

¹*School of Natural Sciences, Far Eastern Federal University,
Vladivostok, Russian Federation*

²*Institute of Applied Mathematics,
Far Eastern Branch, Russian Academy of Science,
Vladivostok, Russian Federation*

³*Department of Physics, Tokyo Metropolitan University,
Hachioji, Tokyo 192-0397, Japan*

(Dated: October 1, 2018)

We study diluted antiferromagnetic Ising models on triangular and kagome lattices in a magnetic field, using the replica-exchange Monte Carlo method. We observe *seven* and *five* plateaus in the magnetization curve of the diluted antiferromagnetic Ising model on the triangular and kagome lattices, respectively, when a magnetic field is applied. These observations contrast with the two plateaus observed in the pure model. The origin of multiple plateaus is investigated by considering the spin configuration of triangles in the diluted models. We compare these results with those of a diluted antiferromagnetic Ising model on the three-dimensional pyrochlore lattice in a magnetic field pointing in the [111] direction, sometimes referred to as the "kagome-ice" problem. We discuss the similarity and dissimilarity of the magnetization curves of the "kagome-ice" state and the two-dimensional kagome lattice.

PACS numbers: 75.40.Mg, 75.50.Lk, 64.60.De

I. INTRODUCTION

Geometrical frustration, a phenomenon associated with structural topology, has recently generated considerable interest. Spin-ice materials, such as pyrochlores $\text{Dy}_2\text{Ti}_2\text{O}_7$ and $\text{Ho}_2\text{Ti}_2\text{O}_7$, have attracted particular attention [1–3]. In these materials, the magnetic ions (Dy^{3+} or Ho^{3+}) occupy sites in a pyrochlore lattice formed of corner-sharing tetrahedra. Their local crystal-field environment causes their magnetic moments to orient along the directions connecting the centers of adjacent tetrahedra at low temperatures. In the low-temperature spin-ice state, the magnetic moments are highly constrained locally and obey the so-called "ice rules", whereby two spins point in and two spins point out of each tetrahedron of the pyrochlore lattice. This two-in two-out spin configuration is analogous to hydrogen atoms in water ice [4].

The effects of magnetic field on the spin-ice materials, in particular the formation of magnetization plateaus, have been studied both theoretically [5–7] and experimentally [8–12]. The effects of dilution on frustration were studied by Ke *et al.* [13] in spin-ice materials. In those studies, magnetic ions Dy or Ho were replaced by nonmagnetic Y ions. The experiments revealed a non-monotonicity in the zero-point entropy, considered as a

function of the dilution concentration. Further studies of the dilution-related effects have also been reported [14–16].

Quite recently, Peretyatko, Nefedev, and Okabe [17] studied the effects of a magnetic field on diluted spin-ice materials in order to elucidate the interplay of dilution and magnetic field. They observed *five* plateaus in the magnetization curve of the diluted nearest-neighbor spin-ice model on the pyrochlore lattice when a magnetic field was applied in the [111] direction. This effect contrasts with the case of a pure (i.e. nondiluted) model, which displays two plateaus. The origin of the *five* plateaus was investigated by considering the spin configuration of two corner-sharing tetrahedra in a diluted model.

One question of interest is whether the existence of multiple steps in the magnetization curve is specific to the diluted model, applied to the three-dimensional (3D) pyrochlore lattice. Another question is what happens in the magnetization curve of diluted antiferromagnetic (AFM) Ising models of two-dimensional (2D) frustrated lattices. The purpose of the present paper is to study the diluted AFM Ising model in the presence of a magnetic field, in the case of triangular and kagome lattices. The calculation for the 2D models is the same as for the pyrochlore lattice. We performed a similar analysis of the origin of multiple plateaus for the case of the pyrochlore lattice, considering the spin configuration in a triangle instead of a tetrahedron.

The pyrochlore lattice can be regarded as an alternating sequence of kagome and triangular layers that become effectively decoupled by a magnetic field oriented along the [111] direction. In this model, the Zeeman energy is expressed as $-\mathbf{h} \cdot \mathbf{d}_{\kappa(i)}$, where $\mathbf{d}_{\kappa(i)}$ is a unit vector of each

* soldatov`ks@students.dvfu.ru

† peretyatko.aa@dvfu.ru

‡ nefedev.kv@dvfu.ru

§ okabe@phys.se.tmu.ac.jp

spin pointing one of the four corners of tetrahedron from the center [7, 17]. When the magnetic field is applied in the [111] direction, say, $\mathbf{h} = h\mathbf{d}_0$, $\mathbf{h} \cdot \mathbf{d}_{\kappa(i)}$ becomes h for apical spins with $\mathbf{d}_{\kappa(i)} = \mathbf{d}_0$, but $-(1/3)h$ for other spins. The spins in the triangular layers, apical spins, are fixed when the magnetic field is applied in this direction. The behavior of the spins in the kagome layers is therefore of significant interest, and is sometimes referred to as the "kagome-ice" problem. It is instructive to study the similarity and dissimilarity between the magnetization curves of the "kagome-ice" state and the 2D kagome lattice.

In this study, we applied the diluted AFM Ising model to the triangular and kagome lattices in a magnetic field. We compare the results with those of the pyrochlore lattice. Our simulations were based on the replica-exchange Monte Carlo method [18] to avoid the system becoming trapped in local-minimum configurations.

The paper is organized as follows: Section II describes the model and the method. The results are then presented and discussed in Sec. III. Section IV concludes with a summary and discussion.

II. MODEL AND SIMULATION METHOD

We studied the AFM Ising model in a magnetic field, applied to 2D triangular and kagome lattices. The corresponding Hamiltonian is given by

$$H = J \sum_{\langle i,j \rangle} \sigma_i \sigma_j - h \sum_i \sigma_i, \quad (1)$$

where $J(> 0)$ represents the AFM coupling, h is the magnetic field, σ_i are the Ising spins ($\sigma_i = \pm 1$), and $\langle i, j \rangle$ denotes a nearest-neighbor pair. Triangular and kagome lattices are illustrated in Fig. 1, for convenience. We here focus on the effects of site dilution on the frustrated AFM Ising models. The Hamiltonian then becomes

$$H = J \sum_{\langle i,j \rangle} c_i c_j \sigma_i \sigma_j - h \sum_i c_i \sigma_i, \quad (2)$$

where c_i are the quenched variables ($c_i = 1$ or 0) and the concentration of vacancies is denoted by x .

We use the Monte Carlo simulation in the present study. The replica-exchange Monte Carlo method [18] is particularly effective in avoiding local-minimum traps. In a previous study, which considered the AFM Ising model on the pyrochlore lattice in a magnetic field applied in the [111] direction [17], the replica-exchange method was successfully applied. We here employ the same simulation method. We perform the replica exchange of both temperature and magnetic field. After each Monte Carlo step of single spin updates, replica exchanges are carried out. When we exchange the inverse temperatures β_1 and β_2 of two replicas, we use a transition probability based

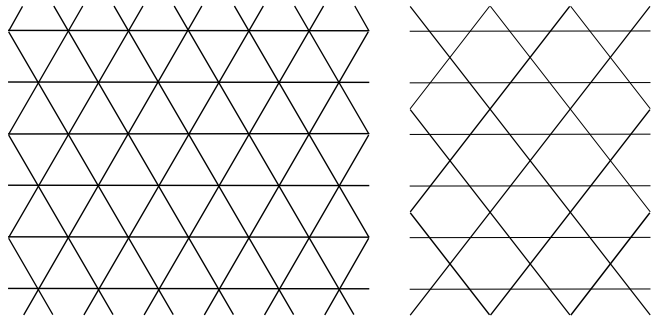


FIG. 1. Illustrations of the triangular lattice (left) and the kagome lattice (right).

on the relative Boltzmann weight, such as

$$\begin{aligned} & \exp[-(\beta_1 E_2 + \beta_2 E_1) + (\beta_1 E_1 + \beta_2 E_2)] \\ & = \exp[(\beta_1 - \beta_2)(E_1 - E_2)]. \end{aligned}$$

Here, E_1 and E_2 are the total energies of two replicas. When we exchange the magnetic fields h_1 and h_2 , the relative Boltzmann weight becomes

$$\begin{aligned} & \exp[-\beta(h_1 E_2^{(Z)} + h_2 E_1^{(Z)}) + \beta(h_1 E_1^{(Z)} + h_2 E_2^{(Z)})] \\ & = \exp[\beta(h_1 - h_2)(E_1^{(Z)} - E_2^{(Z)})], \end{aligned}$$

where $hE^{(Z)}$ is the Zeeman energy part. The calculation may involve many replicas of several temperatures and several magnetic fields. In the present simulation, we treated 486 replicas of 81 magnetic fields and 6 temperatures simultaneously for the triangular lattice, and 336 replicas of 56 magnetic fields and 6 temperatures for the kagome lattice.

The simulation of the AFM Ising model on the triangular lattice considered systems of size $L \times L$ with periodic boundary conditions, with $L = 48$ ($N = 2304$) and $L = 96$ ($N = 9216$). For the kagome lattice of size $L \times (3/2)L$, we used $L = 48$ ($N = 3456$) and $L = 96$ ($N = 13824$). The dilution concentrations x were $x = 0.0$ (pure), 0.1, 0.2, 0.4, 0.6, and 0.8. We discarded the first 5,000 Monte Carlo Steps (MCSs) to avoid the effects of initial configurations, and used the next 50,000 MCSs to generate the measurements. Statistical errors were estimated by calculating averages over 20 samples for each size and each x value.

III. RESULTS

A. Triangular lattice

We first consider the results for the triangular lattice. The averaged values of the magnetization $m = M/N$ with $M = \sum_i \sigma_i$ for the pure model ($x = 0.0$) are plotted in Fig. 2 as a function of the applied field h expressed in units of J . The system size is $L = 96$ ($N = 9216$). The temperatures are $T/J = 0.05, 0.1, 0.15, 0.2, 0.25$, and

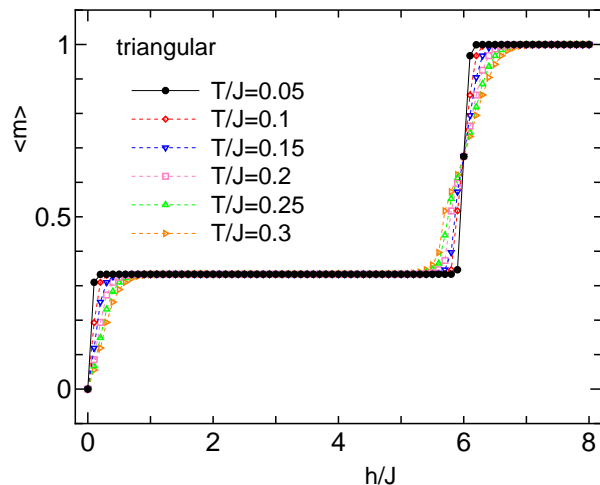


FIG. 2. Magnetization curve for the AFM Ising model on the triangular lattice. The system size is $L = 96$ ($N = 9216$), and the temperatures are $T/J = 0.05, 0.1, 0.15, 0.2, 0.25$ and 0.3 .

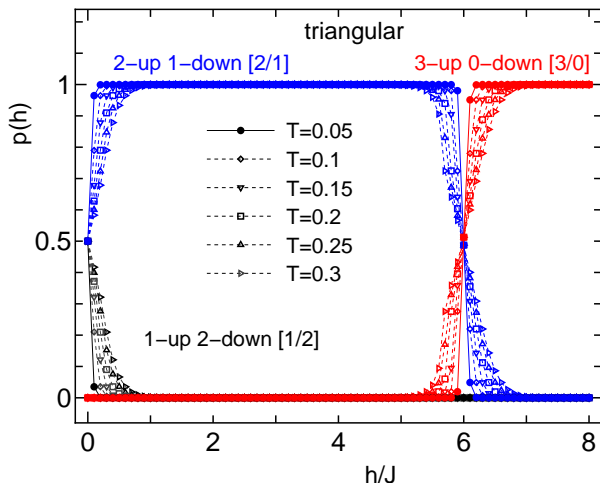


FIG. 3. Proportions of the types of spin configurations in the triangle for the AFM Ising model on the triangular lattice in a magnetic field. The system size is $L = 96$ ($N = 9216$), and the temperatures are $T/J = 0.05, 0.1, 0.15, 0.2, 0.25$, and 0.3 .

0.3. Averages were computed over 20 samples with different random-number sequences. The statistical errors are smaller than the size of the marks. The size dependence is small for large enough sizes, such as $L = 48$ and $L = 96$. We see an $m = 1/3$ plateau for $h/J < 6$, and the jump becomes smoother with increasing temperature.

Figure 3 displays the proportions of the types of spin configurations within the triangle, for the AFM Ising model on the triangular lattice in the magnetic field. There are 18432 triangles for $L = 96$, and the proportions of the types of spin configurations were measured for 50,000 MCSs. The type of a given spin configurations was characterized in terms of the numbers of up (+1)

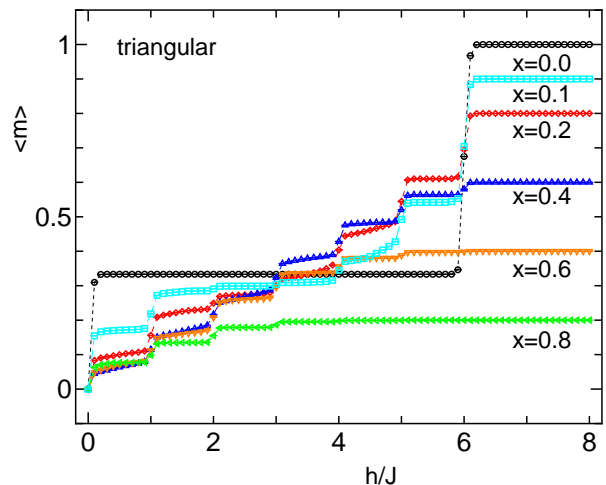


FIG. 4. Magnetization curve for the diluted AFM Ising model on the triangular lattice. The system size is $L = 96$ ($N = 9216$), and the temperature is $T/J = 0.05$. The dilution concentrations (x) are 0.0, 0.1, 0.2, 0.4, 0.6 and 0.8.

spins and down (-1) spins within the triangle. There is a clear transition from the 2-up 1-down configuration to the 3-up 0-down configuration at $h/J = 6$. This transition becomes smoother with increasing temperature.

The magnetization curve for the diluted AFM Ising model on the triangular lattice is plotted in Fig. 4. The system size is $L = 96$ ($N = 9216$), and the temperature is $T/J = 0.05$. The dilution concentrations (x) are 0.0, 0.1, 0.2, 0.4, 0.6 and 0.8. Averages were calculated over 20 random samples. The error bars in the figure are smaller than the size of marks. The statistical errors, obtained by averaging over 20 random samples, become very small when the system size is as large as $L = 96$ ($N = 9216$).

We observe seven plateaus in the magnetization curve of diluted systems; for $h/J < 1$, $1 < h/J < 2$, $2 < h/J < 3$, $3 < h/J < 4$, $4 < h/J < 5$, $5 < h/J < 6$, and $h/J > 6$. In contrast, the pure case shows only two plateaus, located on either side of $h/J = 6$. The results shown correspond to $T/J = 0.05$. At higher temperatures, the magnetic step between the plateaus becomes smoother. The magnetization m saturates at $(1 - x)$.

In an earlier study of the diluted triangular-lattice AFM Ising model in a magnetic field, Yao [19] obtained the magnetization curve for the diluted system of weak dilution regions using the Wang-Landau method. Žukovič *et al.* [20] used the effective-field theory to study the diluted AFM Ising model. Multiple plateaus were reported in both studies. Effects of thermal fluctuations were also discussed [20, 21].

In the case of the pure model, the spin configuration of the triangle changes from the 2-up 1-down configuration to the 3-up 0-down configuration when the magnetic field is applied. On the contrary, the spin configuration becomes more complex in diluted systems. The magnetic-field dependence of the spin configuration is plotted in

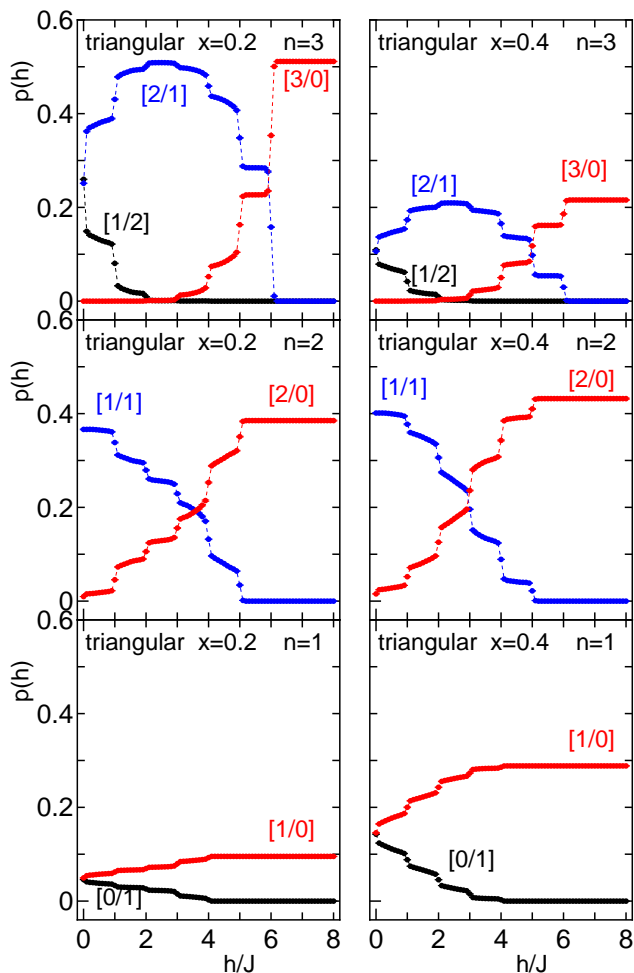


FIG. 5. Proportions of the types of spin configurations in the triangle for the diluted AFM Ising model on the triangular lattice in a magnetic field. The system size is $L = 96$ ($N = 9216$), and the temperature is $T/J = 0.05$. The dilution concentrations (x) are 0.2 (left) and 0.4 (right). The number of spins n in the triangle is 3, 2, and 1 for the top, middle, and bottom panel, respectively.

Fig. 5 for a system size $L = 96$ ($N = 9216$), and the temperature $T/J = 0.05$. The dilution concentrations (x) are 0.2 and 0.4. Averaging was performed over 20 random systems. There are 18432 triangles for $L = 96$, and the number of spins in a triangle, n , becomes $n = 3, 2, 1$, or 0 for the diluted systems.

The top panel of Fig. 5 corresponds to $n = 3$. There are $n = 3$ spins for approximately 51% of all triangles when $x = 0.2$, and approximately 22% when $x = 0.4$. The change from the 2-up 1-down configuration, $[2/1]$, to the 3-up 0-down configuration, $[3/0]$, is observed at $h/J = 6$ as in the pure case. However, the proportions of $[2/1]$ and $[3/0]$ also change at $h/J = 1, 2, 3, 4$, and 5. For the low- h region, the 1-up 2-down configuration, $[1/2]$, remains.

The middle panel of Fig. 5 corresponds to $n = 2$. One

TABLE I. The local energy of the spin configuration in the triangle for the triangular lattice. The spin numbers n are 3, 2, and 1. An edge is shared with two triangles, and a corner is shared with six triangles.

config.	n spins	up	down	energy
$[3/0]$	3	3	0	$3(J/2) - 3(h/6)$
$[2/1]$		2	1	$-(J/2) - (h/6)$
$[1/2]$		1	2	$-(J/2) + (h/6)$
$[2/0]$	2	2	0	$(J/2) - 2(h/6)$
$[1/1]$		1	1	$-(J/2)$
$[1/0]$	1	1	0	$-(h/6)$
$[0/1]$		0	1	$+(h/6)$

spin is deleted from the triangle. The partial transition from the 1-up 1-down configuration, $[1/1]$, to the 2-up 0-down configuration, $[2/0]$, is observed.

The bottom panel of Fig. 5 corresponds to $n = 1$. Here, two spins are deleted from the triangle. At $h/J = 0$, there are equal proportions of up spins and down spins, whereas the proportion of up spins increases as the magnetic field h increases.

We showed the data of the proportions of the types of spin configurations in the triangle for $x = 0.2$ and $x = 0.4$ in Fig. 5. We see the x dependence. The situation is essentially the same, although the proportions of configurations with smaller n values increase as x increases. For strong dilution, such as $x = 0.8$, many free spins appear, which does not produce a magnetization plateau; the magnetization jump decreases for larger x .

We follow a similar procedure as for the case of the pyrochlore lattice in the $[111]$ magnetic field [17] to elucidate the origin of the seven plateaus in the magnetization curve. We investigate the local energy of the spin configuration in a triangle for $n = 3, 2$, and 1, the results of which are shown in Table I. The local energy for each configuration is given in the last column. An edge, which is related to the exchange energy, is shared by two neighboring triangles, and a corner, which is related to the Zeeman energy, is shared by six triangles.

We consider the energy of six corner-sharing triangles. Figure 6 illustrates the flipping process schematically. The deleted spins are denoted by empty circle. The case where all the six triangles have $n = 3$ is shown in panel (i). When the corner-sharing spin is turned from "down" to "up", the configuration changes from $[2/1]$ to $[3/0]$. From Table I, the crossover magnetic field is calculated by

$$-(J/2) - (h/6) = 3(J/2) - 3(h/6).$$

We then obtain $h_c/J = 6$. If one spin is deleted as in panel (ii), there are four triangles with $n = 3$ and two triangles with $n = 2$. When the corner-sharing spin is turned from "down" to "up", the configuration changes from $(4[2/1] + 2[1/1])$ to $(4[3/0] + 2[2/0])$. From Table I,

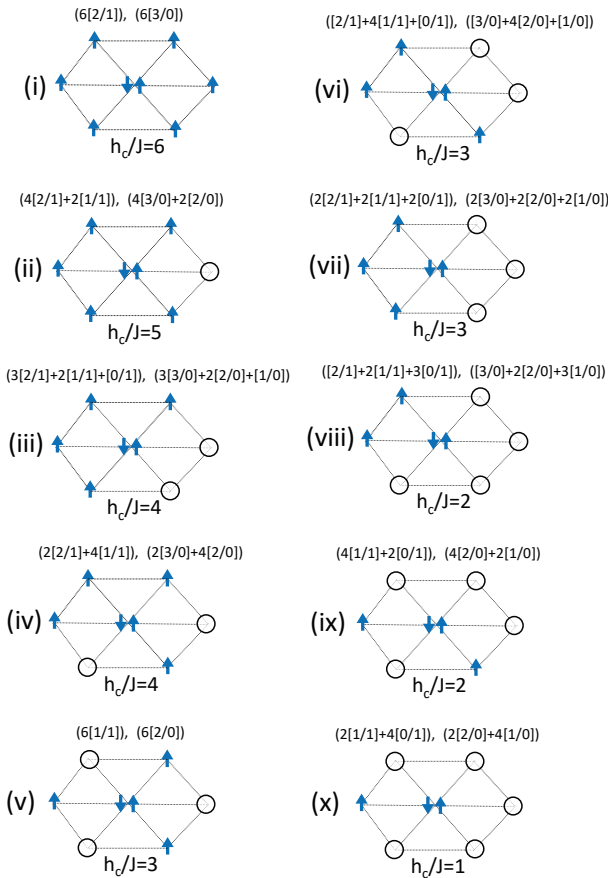


FIG. 6. Schematic illustration of spin flip for the triangular lattice. The up and down spins are denoted by the arrow, whereas the deleted spins are denoted by the empty circle. The crossover values h_c are given there.

the crossover magnetic field is calculated by

$$4(-(J/2) - (h/6)) + 2(-(J/2)) \\ = 4(3(J/2) - 3(h/6)) + 2((J/2) - 2(h/6)).$$

We then obtain $h_c/J = 5$. The deletion of two spins makes us consider two cases: firstly, the change from $(3[2/1]+2[1/1]+[0/1])$ to $(3[3/0]+2[2/0]+[1/0])$, as shown in panel (iii), and secondly, the change from $(2[2/1]+4[1/1])$ to $(2[3/0]+4[2/0])$, as shown in panel (iv). In both cases, the crossover magnetic field is $h_c/J = 4$. The cases where three spins are deleted are shown in panels (v), (vi), and (vii), whereas those where four spins are deleted are shown in panels (viii) and (ix). Panel (x) corresponds to the deletion of five spins. The crossover values h_c , given in Fig. 6, can be obtained in the same manner.

This investigation clearly accounts for the change in the configurations displayed in Fig. 5, which clarifies the origin of the seven magnetization plateaus in Fig. 4. The magnetization step at $h/J = 6$ comes from the situation shown in panel (i) of Fig. 6. When one increases

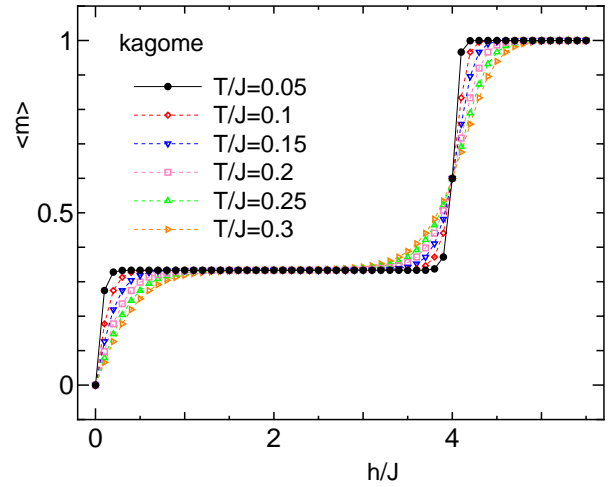


FIG. 7. Magnetization curve for the AFM Ising model on the kagome lattice. The system size is $L = 96$ ($N = 13824$), and the temperatures are $T/J = 0.05, 0.1, 0.15, 0.2, 0.25$ and 0.3 .

the dilution concentration x , the possibility of such spin configurations becomes small. Thus, for strong dilution cases, the magnetization steps at $h/J = 6$ and also at $h/J = 5$ become very small.

B. Kagome lattice

We next consider the kagome lattice. The averaged values of the magnetization $m = M/N$ for the pure model ($x = 0.0$) are plotted as a function of the applied field h in Fig. 7. The system size is here $L = 96$ ($N = 13824$) and the temperatures are $T/J = 0.05, 0.1, 0.15, 0.2, 0.25$, and 0.3 . Averaging was performed over 20 samples with different random-number sequences. The plateau corresponding to $m = 1/3$ appears for $h/J < 4$, but the jump becomes smoother with increasing temperature.

Figure 8 shows the proportions of the different types of spin configurations in a triangle for the AFM Ising model on the kagome lattice in a magnetic field. There are 9216 triangles for $L = 96$, and the proportions of the different types of spin configurations were measured for 50,000 MCSs. The type of spin configurations in a triangle is classified in the same way as for the triangular lattice. There is a clear transition from the 2-up 1-down configuration to the 3-up 0-down configuration at $h/J = 4$. The transition becomes smoother when increasing temperature.

The magnetization curve for the diluted AFM Ising model on the kagome lattice is plotted in Fig. 9. The system size is $L = 96$ ($N = 13824$), and the temperature is $T/J = 0.05$. The dilution concentrations (x) are 0.0, 0.1, 0.2, 0.4, 0.6 and 0.8.

Figure 9 shows five plateaus in the magnetization curves, in the ranges $h/J < 1$, $1 < h/J < 2$, $2 < h/J < 3$,

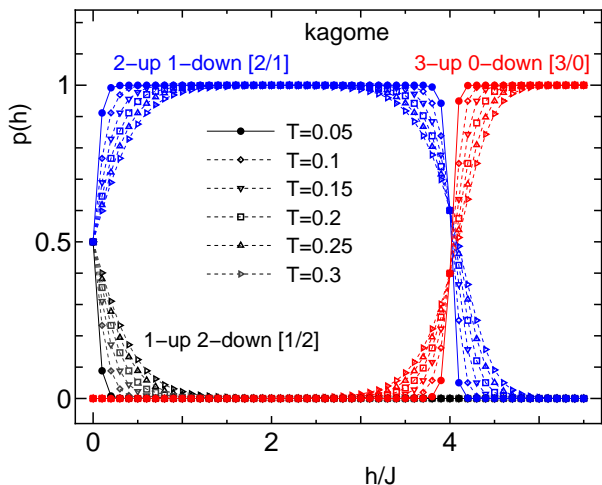


FIG. 8. Proportions of the types of spin configurations in the triangle for the AFM Ising model on the kagome lattice in a magnetic field. The system size is $L = 96$ ($N = 13824$), and the temperatures are $T/J = 0.05, 0.1, 0.15, 0.2, 0.25,$ and 0.3 .

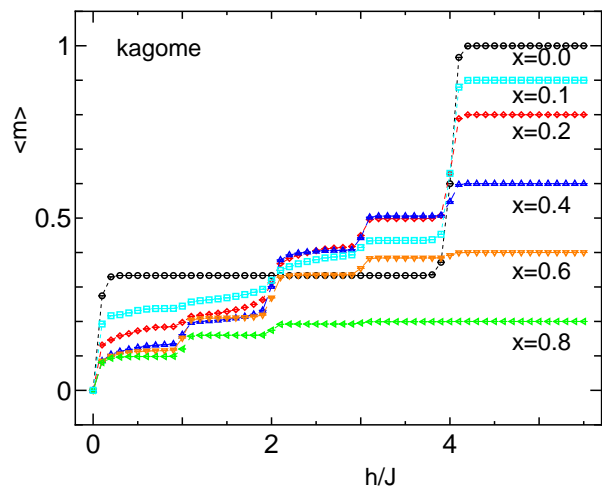


FIG. 9. Magnetization curve for the diluted AFM Ising model on the kagome lattice. The system size is $L = 96$ ($N = 13824$), and the temperature is $T/J = 0.05$. The dilution concentrations (x) are $0.0, 0.1, 0.2, 0.4, 0.6$ and 0.8 .

$3 < h/J < 4$, and $h/J > 4$. This situation contrasts with the pure case, where only two plateaus are observed, on either side of $h/J = 4$. The saturated value of the magnetization m is $(1 - x)$.

The magnetic-field dependence of the spin configuration for the diluted AFM model on the kagome lattice is plotted in Fig. 10. The system size is $L = 96$ ($N = 13824$), and the temperature is $T/J = 0.05$. The dilution concentrations (x) are 0.2 and 0.4 . There are 9216 triangles for $L = 96$, and the number of spins in the triangle, n , becomes $n = 3, 2, 1,$ or 0 for the diluted systems.

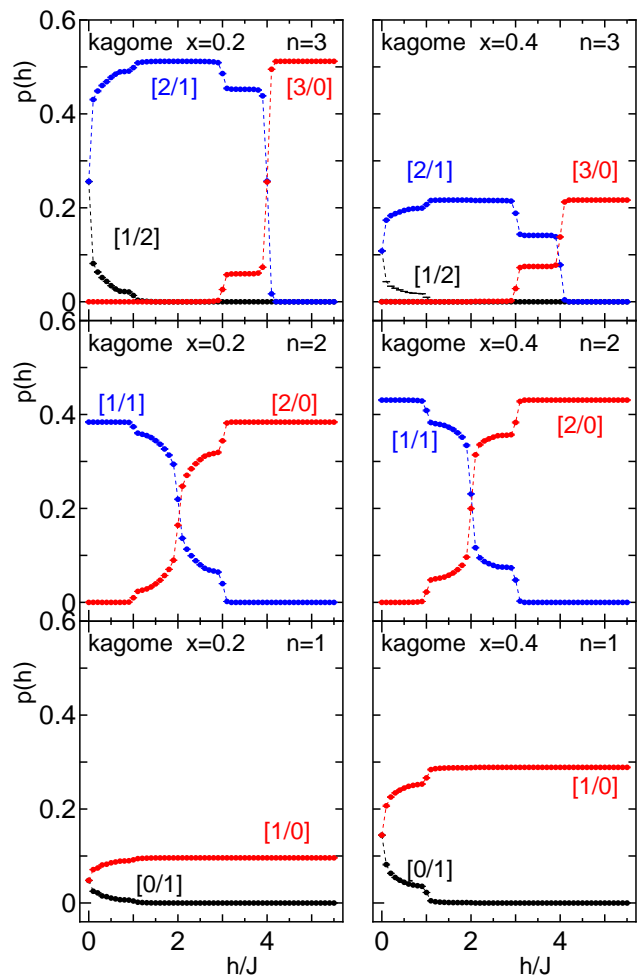


FIG. 10. Proportions of the types of spin configurations in the triangle for the diluted AFM Ising model on the kagome lattice in a magnetic field. The system size is $L = 96$ ($N = 13824$), and the temperature is $T/J = 0.05$. The dilution concentrations (x) are 0.2 (left) and 0.4 (right). The number of spins n in the triangle is $3, 2,$ and 1 for the top, middle, and bottom panel, respectively.

The top panel of Fig. 10 shows the result for $n = 3$, which corresponds to approximately 51% of all the triangles for $x = 0.2$ and approximately 22% for $x = 0.4$ again. A transition from the 2-up 1-down configuration, $[2/1]$, to the 3-up 0-down configuration, $[3/0]$, is observed at $h/J = 4$, as in the pure case. However, the proportions of the $[2/1]$ and $[3/0]$ configurations also change at $h/J = 1, 2,$ and 3 .

The middle panel of Fig. 10 corresponds to $n = 2$. One spin is deleted from the triangle. The partial transition is observed from the 1-up 1-down configuration, $[1/1]$, to the 2-up 0-down configuration, $[2/0]$.

The bottom panel corresponds to $n = 1$, where two spins are deleted from the triangle. At $h/J = 0$, there are equal proportions of up and down spins, whereas the

TABLE II. The local energy of the spin configuration in the triangle for the kagome lattice. The spin numbers n are 3, 2, and 1. An edge is not shared with other triangles, and a corner is shared with two triangles.

config.	n spins	up	down	energy
[3/0]	3	3	0	$3J - 3(h/2)$
[2/1]		2	1	$-J - (h/2)$
[1/2]		1	2	$-J + (h/2)$
[2/0]	2	2	0	$J - 2(h/2)$
[1/1]		1	1	$-J$
[1/0]	1	1	0	$-(h/2)$
[0/1]		0	1	$+(h/2)$

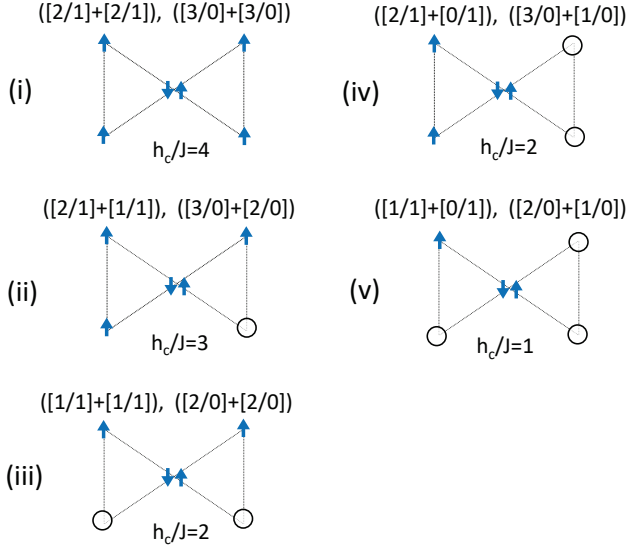


FIG. 11. Schematic illustration of spin flip for the kagome lattice. The up and down spins are denoted by the arrow, whereas the deleted spins are denoted by the empty circle. The crossover values h_c are given there.

proportion of up spins increases with increasing h .

We showed the data of the proportions of the types of spin configurations in the triangle for $x = 0.2$ and $x = 0.4$. The situation is essentially the same, although the proportions of smaller n in the triangle increases when x become larger.

We use the same analysis as above to elucidate the origin of the multiple plateaus in the magnetization curve. The local energies of the spin configuration of the triangle for $n = 3, 2$, and 1 are listed in Table II. An edge, which is related to the exchange energy, is not shared with other triangles, and a corner, which is related to the Zeeman energy, is shared between two triangles.

In the case of the kagome lattice, we consider the energy of two corner-sharing triangles. The flipping process is illustrated schematically in Fig. 11. Deleted spins

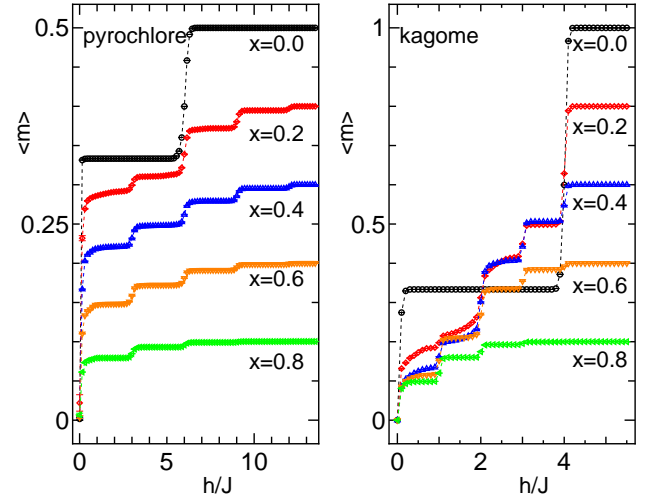


FIG. 12. The comparison of the magnetization curves for the diluted AFM Ising model on the pyrochlore lattice [17] and on the kagome lattice (the present study). In the case of pyrochlore lattice the magnetization is applied in the [111] direction.

are denoted by empty circle. The case where the two triangles have $n = 3$ is shown in panel (i). When the corner-sharing spin is turned from "down" to "up", the configuration changes from [2/1] to [3/0]. From Table II, the crossover magnetic field is calculated by

$$-J - (h/2) = 3J - 3(h/2).$$

We then obtain $h_c/J = 4$. If one spin is deleted as shown in panel (ii), one triangle has $n = 3$ and the other triangle has $n = 2$. When the corner-sharing spin is turned from "down" to "up", the configuration changes from ([2/1]+[1/1]) to ([3/0]+[2/0]). From Table II, the crossover magnetic field is calculated by

$$\begin{aligned} &(-J - (h/2)) + (-J) \\ &= (3J - 3(h/2)) + (J - 2(h/2)). \end{aligned}$$

We then obtain $h_c/J = 3$. Two cases arise when two spins are deleted: (2[1/1]) changes to (2[2/0]), as shown in panel (iii), and ([2/1]+[0/1]) changes to ([3/0]+[1/0]), as shown in panel (iv). In both cases, the crossover magnetic field is given by $h_c/J = 2$. The case where three spins are deleted is shown in panel (v). The corresponding crossover values h_c are obtained in the same way as before, and are given in Fig. 11.

This analysis explains the change in the configurations given in Fig. 10. The origin of the five magnetization plateaus in Fig. 9 is thus clearly elucidated, as for the triangular lattice.

C. Comparison with "kagome-ice"

The pyrochlore lattice can be regarded as consisting of alternating kagome and triangular layers that become

effectively decoupled by a magnetic field in the [111] direction. Since the spins in the triangular layers are fixed, as explained in Sec. I, Introduction, the behavior of the spins in the kagome layers has attracted significant interest. This problem is sometimes referred to as the "kagome-ice" problem [9, 10]. It is interesting to compare the behavior of the "kagome-ice" with that of the AFM Ising model on a 2D kagome lattice.

Figure 12 compares the magnetization curves of the diluted AFM Ising models on the pyrochlore lattice [17] and on the kagome lattice (the present study). In the case of the "kagome-ice" state for the pure model ($x = 0$), the magnetization saturates at $m = 1/2$, with an intermediate plateau at $m = 1/3$. It comes from a complex structure of the spin-ice model on the pyrochlore lattice. When a magnetic field is applied in the [111] direction, the spins on the [111] positions are fixed as 1, but other spins take either $+(1/3)$ or $-(1/3)$ [17]. The magnetization of the kagome lattice saturates at $m = 1$ for the pure case ($x = 0$), with an intermediate plateau at $m = 1/3$.

The diluted model of the "kagome-ice" state displays new steps at different magnetic fields relative to the pure model ($h/J = 6$), namely at $h/J = 3, 9$, and 12 . In the case of the kagome lattice, new steps appear at $h/J = 1, 2$, and 3 ; the pure case shows a single step at $h/J = 4$. Although there are five plateaus in the magnetization curves of the diluted models in the case of both the pyrochlore and kagome lattices, the positions of the new transitions are different. The plateaus result from the competition between the exchange and Zeeman energies, which differ in the pyrochlore (Table I of Ref. [17]) and kagome lattices (Table II of the present study). There are therefore both similarities and dissimilarities between the magnetization curves of the diluted model for the "kagome-ice" state and for the kagome lattice.

IV. SUMMARY AND DISCUSSIONS

To summarize, we studied diluted AFM Ising models on triangular and kagome lattices in a magnetic field using the replica-exchange Monte Carlo method for both

temperature and magnetic field. We observed *seven* and *five* plateaus in the resulting magnetization curves for triangular and kagome lattices, respectively. These results contrast with the case of the pure model, which displays only two plateaus. The spin configuration within triangles was investigated, which clearly accounted for the origin of multiple magnetization plateaus in the diluted models. The present results were compared with those of the diluted AFM Ising model on the 3D pyrochlore lattice in a magnetic field along the [111] direction, a scenario sometimes referred to as the "kagome-ice" problem. We discussed the similarity and dissimilarity between the magnetization curves for the "kagome-ice" state and for the 2D kagome lattice. Both models have five magnetization plateaus, but the positions of magnetization steps are different. It is because the condition of the competition between the exchange and Zeeman energies are different in both models.

These theoretical results highlight the rich variety of effects expected to result from the interplay of dilution and magnetic field in frustrated systems. Spin-ice materials on the pyrochlore lattice have attracted particular attention, and multiple magnetization plateaus in the diluted model were theoretically proposed quite recently [17]. The present study on the triangular and kagome lattices revealed that this phenomenon is general in diluted frustrated systems. Future experimental studies will be needed to demonstrate them in natural and artificial spin-ice materials [22].

ACKNOWLEDGMENT

We thank Vitalii Kapitan, Yuriy Shevchenko, and Hiromi Otsuka for valuable discussions. The computer cluster of Far Eastern Federal University and the equipment of Shared Resource Center "Far Eastern Computing Resource" IACP FEB RAS were used for computation. This work was supported by a Grant-in-Aid for Scientific Research from the Japan Society for the Promotion of Science, Grants No. JP25400406 and No. JP16K05480.

-
- [1] M. J. Harris, S. T. Bramwell, D. F. McMorrow, T. Zeiske, and K.W. Godfrey, Phys. Rev. Lett. **79**, 2554 (1997).
 - [2] A. P. Ramirez, A. Hayashi, R. J. Cava, R. Siddharthan, and B. S. Shastry, Nature (London) **399**, 333 (1999).
 - [3] S. T. Bramwell and M. J. P. Gingras, Science **294**, 1495 (2001).
 - [4] L. Pauling, J. Am. Chem. Soc. **57**, 2680 (1935).
 - [5] M. J. Harris, S. T. Bramwell, P. C. W. Holdsworth, and J. D. M. Champion, Phys. Rev. Lett. **81**, 4496 (1998).
 - [6] R. Moessner and S. L. Sondhi, Phys. Rev. B **68**, 064411 (2003).
 - [7] S. V. Isakov, K. S. Raman, R. Moessner, and S. L. Sondhi, Phys. Rev. B **70**, 104418 (2004).
 - [8] K. Matsuhira, Z. Hiroi, T. Tayama, S. Takagi, and T. Sakakibara, J. Phys.: Condens. Matter **14**, L559 (2002).
 - [9] Z. Hiroi, K. Matsuhira, S. Takagi, T. Tayama, and T. Sakakibara, J. Phys. Soc. Jpn. **72**, 411 (2003).
 - [10] T. Sakakibara, T. Tayama, Z. Hiroi, K. Matsuhira, and S. Takagi, Phys. Rev. Lett. **90**, 207205 (2003).
 - [11] R. Higashinaka, H. Fukazawa, and Y. Maeno, Phys. Rev. B **68**, 014415 (2003).
 - [12] H. Fukazawa, R. G. Melko, R. Higashinaka, Y. Maeno, and M. J. P. Gingras, Phys. Rev. B **65**, 054410 (2002).
 - [13] X. Ke, R. S. Freitas, B. G. Ueland, G. C. Lau, M. L. Dahlberg, R. J. Cava, R. Moessner, and P. Schiffer, Phys. Rev. Lett. **99**, 137203 (2007).

- [14] T. Lin, X. Ke, M. Thesberg, P. Schiffer, R. G. Melko, and M. J. P. Gingras, *Phys. Rev. B* **90**, 214433 (2014).
- [15] S. Scharffe, O. Breunig, V. Cho, P. Laschitzky, M. Vallador, J. F. Welter, and T. Lorenz, *Phys. Rev. B* **92**, 180405(R) (2015).
- [16] Y. Shevchenko, K. Nefedev, and Y. Okabe, accepted for publication in *Phys. Rev. E*, arXiv:1705.05446 (2017).
- [17] A. Peretyatko, K. Nefedev, and Y. Okabe, *Phys. Rev. B* **95**, 144410 (2017).
- [18] K. Hukushima and K. Nemoto, *J. Phys. Soc. Jpn.* **65**, 1604 (1996).
- [19] X. Yao, *Solid State Commun.* **150**, 160 (2010).
- [20] M. Žukovič, M. Borovský, and A. Bobák, *Phys. Lett. A* **374**, 4260 (2010).
- [21] M. Borovský, M. Žukovič, and A. Bobák, *Acta Physica Polonica A* **126**, 16 (2014).
- [22] Y. Qi, T. Brintlinger, and J. Cumings, *Phys. Rev. B* **77**, 094418 (2008).